

On the effects of the stellar magnetic field on the structure of T Tauri accretion discs

Y. Ultchin,¹ O. Regev¹ and G. A. Wynn²

¹ *Physics Department, Technion - Israel Institute of Technology, Haifa 32000, Israel*

² *Astronomy Group, Leicester University, University Road, Leicester LE1 7RH*

Accepted ——. Received ——; in original form ——.

ABSTRACT

The structure of accretion discs around magnetic T Tauri stars is numerically calculated using a particle hydrodynamical code, in which magnetic interaction is included in the framework of King’s dimagnetic blob accretion model. Setting up the calculation so as to simulate the density structure of a quasi-steady disc in the equatorial plane of a T Tauri star, we find that the central star’s magnetic field typically produces a central hole in the disc and spreads out the surface density distribution. We argue that this result suggests a promising mechanism for explaining the unusual flatness (IR excess) of T Tauri accretion disc spectra.

Key words: accretion, accretion discs – stars: pre-main-sequence – stars: magnetic fields.

1 INTRODUCTION

It is now quite widely accepted that in the formation process of low-mass ($M \lesssim 2M_{\odot}$) stars, a disc accretion phase is typically present (see Hartmann 1998 for an extensive review and references). In particular, the classical T Tauri stars (CTTS) are thought to be still surrounded by discs and the emission properties of some typical objects suggest that these discs are not merely “passive” dust bodies, irradiated by the central star, but are rather bona-fide energy producing, viscous accretion discs, similar to the ones present in mass transferring close binary systems, and whose modeling dates back to the classical works of Shakura & Sunyaev (1973) and Lynden-Bell & Pringle (1974). Because of their ubiquity and

of some interesting theoretical challenges they pose, accretion discs have remained at the centre stage of astrophysical research (see e.g. Frank, King & Raine 1992; Papaloizou & Lin 1995; Lin & Papaloizou 1996 for reviews).

One particular issue in this context is the fact that in many CTTS the measured spectrum presents an unusually high emission in the infra red (called IR excess), far more than expected from disc reprocessing of stellar light or viscous heating of the disc (see Bertout 1989, Beckwith et al. 1990, Hartmann et al. 1994). Our wish to investigate this problem, as well as some other facets of CTTS discs, has been the main motivation for the work reported on in this paper. It consists of setting up a numerical calculation of the properties of an accretion disc around magnetic CTTS, using a scheme of magnetic interaction, originally proposed in the context of diamagnetic accretion by King (1993).

This description of the magnetic interaction assumes that as material moves through the magnetosphere it interacts with the local magnetic field via a velocity dependent acceleration (force per unit mass, f_{mag}) of the form:

$$f_{\text{mag}} = -K [\mathbf{u} - \mathbf{u}_f]_{\perp}, \quad (1)$$

where \mathbf{u} and \mathbf{u}_f are the velocities of the material and magnetic field lines respectively, K is a suitable "magnetic drag" coefficient (see below) and the suffix \perp refers to the vector component perpendicular to the field line. The magnetic acceleration, as expressed in equation 1, is intended to represent the dominant term of the magnetic interaction, with K containing the relevant parameters determining the effective magnetic time-scale.

Within the above description (1) there are still a number of different possibilities to model the inner disc - magnetosphere interaction. In this paper we shall use the diamagnetic blob accretion (DBA) model, although it is possible to formulate the diametrically opposite case (complete magnetic penetration of the disc) in the general form (1) as well. Wynn, Leach & King (2001) show how to calculate the appropriate coefficient K for the latter case and we plan to repeat our calculations in the future, using this prescription.

In the DBA approach one assumes that the fluid constituting the accretion flow, i.e. the disc and its surroundings, is composed of blobs immersed in a dilute interblob plasma (see Aly & Kuipers 1990). The blobs behave diamagnetically in the presence of the stellar magnetic field and thus suffer a surface drag force acting on them. The model has since its introduction been applied to various systems, notably to the intermediate polar class of cataclysmic variables (CV). Wynn & King (1995) and Wynn, King & Horne (1997)

incorporated the diamagnetic drag force into a particle hydrodynamical numerical code (HYDISC), originally developed by Whitehurst (1988) to simulate the accretion disc in non-magnetic close binary systems. They found important properties of the white dwarf's spin evolution and its effect on the disc and explicitly applied their findings to the moderately magnetic CV AE Aqr. A more recent study using this approach was its application to the system EX Hya (King & Wynn 1999).

The DBA approach was extended to the study of accreting T Tauri stars for the first time by King & Regev (1994), hereafter KR. They performed calculations of *individual* blob (that is, ballistic) orbits, including the interaction with magnetic loops of the central star and have shown that this mechanism can eject blobs from the system, in directions pointing away from the disc plane. By estimating the angular momentum thus expelled and including it in the overall angular momentum budget KR found that a stellar spin equilibrium value is compatible with the observations (i.e. \sim an order of magnitude less than the breakup value) if the magnetic loops extend to a few stellar radii. Pearson & King (1995), hereafter PK, generalised the above work into a N -particle simulation, in a similar manner to the one mentioned above for CVs. This work also focused on the issue of the slow observed T Tauri spin rates and confirmed the idea that such equilibrium spin rates can be achieved by the expulsion of matter from the disc until the corotation radius (see below) coincides with the edge of the magnetic loop. The additional new finding, not anticipated by KR, of this work was that the ejection of material comes to a halt as the star approaches its spin equilibrium value.

The problem of the slow spin rates and rotational evolution of T Tauri stars as a result of the star's magnetic interaction with its accretion disc has been also approached, in a number of works, by analytical and semi-analytical methods, that is, stopping short of multi-dimensional numerical simulations. Königl (1991), Cameron & Campbell (1993) and Armitage & Clarke (1996) used quite different approaches and all found that a stellar dipole magnetic field of strength $\lesssim 1$ kG is able to regulate the stellar spin to a quasi-static value, in the observed range. In the process of the magnetic interaction the inner accretion disc gets disrupted and the inner (abrupt) termination radius of the disc was estimated in the above papers.

KR and PK used the DBA approach focusing on the ejection of mass from the disc, in an effort to link the low spin rates of T Tauri stars with outflows from young stellar objects (YSO) within a unified scenario. In the present work we utilise the DBA model in

the calculation of the properties of the steady (or quasi-steady) accretion disc itself, that is, the material that remains close to the equatorial plane while spiraling in due to viscous torques, *after* the spin period has already stabilised. Some peculiarities of T Tauri *light-curves* (i.e. the temporal luminosity variations) have already been treated using a model based on single blob ballistic orbits, which leave the the disc plane but ultimately return and impinge on the disc surface (Ultchin et al. 1997). In order to investigate whether the DBA model is consistent with some of the basic properties of T Tauri *spectra* (see Bertout 1989 and references therein) and in particular the above mentioned IR excess, we have performed numerical simulations using a code based on HYDISC, suitably modified so as to adapt it for the problem at hand.

This paper is organised as follows. In the next section we discuss the basics of blob dynamics and estimate the relevant time-scales. §3 describes the numerical code used in the accretion flow simulation and the procedure for finding the spectrum emitted by such flows. In §4 the results of our simulations for a score of parameter values are described in some detail and finally, §5 summarises this work in comparison to the results of other approaches.

2 DIAMAGNETIC ACCRETION FLOW DYNAMICS

Following KR and PK we model the material of a T Tauri disc as being composed of gas blobs immersed in a tenuous interblob plasma. These blobs are assumed to behave diamagnetically in the presence of the magnetic field of the central star, which threads the plasma. Drell, Folley & Ruderman (1965) showed that the typical time-scale on which a diamagnetic object of mass m (i.e. a blob) loses energy, when it moves in a magnetic field B , is

$$t_d = \frac{c_A m}{B^2 l_b^2} \quad (2)$$

where $c_A = \sqrt{B^2/(4\pi\rho_p)}$ is the Alfvén speed of the interblob plasma, whose density is ρ_p , and l_b is the blob size. There is a minimum condition on the conductivity for this equation to hold and, as it was shown by KR, this condition is satisfied for all reasonable parameters in the conditions appropriate for T Tauri accretion.

This allows to cast the diamagnetic force per unit mass, acting on a blob, into one simple formula, whose form is in accordance with equation 1:

$$\mathbf{f}_d = -K_d [\mathbf{u}_b - \mathbf{u}_f]_{\perp} \hat{\mathbf{n}}, \quad (3)$$

where $K_d = 1/t_d$ (see below) is the diamagnetic drag coefficient. The magnetic drag force obviously vanishes if the blob velocity \mathbf{u}_b relative to the velocity of the local field line \mathbf{u}_f is *parallel* to the field lines, it is proportional to the perpendicular (to the local field) component of this relative velocity and is directed in the normal direction $\hat{\mathbf{n}}$ to the field. This is the meaning of the shorthand vector notation in equation 3. Its explicit component form will be given below.

Assuming that the magnetic field rotates with the star and does not change on the time-scale of interest, the above equation is best explicitly written in the frame of reference *rotating with* the central star and had the form

$$\mathbf{f}_d = -K_d [\mathbf{v} - (\mathbf{v} \cdot \mathbf{b})\mathbf{b}], \quad (4)$$

where \mathbf{v} is the blob velocity *in the rotating frame*, that is, relatively to the field lines, and \mathbf{b} is a unit vector in the local field direction (see KR).

Substituting explicitly the above form of c_A and $m = l_b^3 \rho_b$, where ρ_b is the blob density, in the drag coefficient one gets

$$K_d(\mathbf{x}) = 2\sqrt{\pi} \rho_p^{1/2} (\rho_b l_b)^{-1} B \equiv K f(\mathbf{x}), \quad (5)$$

where the second equality parametrizes K_d in terms of a constant coefficient K and a spatially dependent (\mathbf{x} denotes the position vector) function, which is of order 1. The blob parameters and their space dependence, as well as the plasma density, are rather uncertain. The only variable which can be explicitly written is the magnetic field (in the approximation that it is fixed in the rotating frame, that is, anchored to the star), because it can be chosen a priori.

In this work we shall mainly use a dipolar magnetic field configuration and group, for the sake of convenience, all the other variables into a single fixed parameter, incorporating in it most of our ignorance of the complex plasma instabilities, which are supposed to create and shape the blobs. Within this framework we have

$$K_d = K (R/R_*)^{-3} [1 + 3(z/R)]^{1/2}, \quad (6)$$

in cylindrical coordinates (R, z) whose z axis coincides with the dipole axis. R_* is the stellar radius and

$$K = \sqrt{\pi} \rho_p^{1/2} (\rho_b l_b)^{-1} B_0, \quad (7)$$

where B_0 is the polar field strength. This K is assumed to be constant and will serve as a parameter of our problem. For a discussion of the different options to chose K_d see e.g. Wynn, King & Horne (1997).

We focus in this work on the case of an *aligned* dipole, that is, when the dipole axis coincides with the disc axis, but will briefly discuss (in §4.3) the inclined dipole case as well.

The magnetic drag term has to be added to the blob equations of motion, which include also gravitational, centrifugal and coriolis terms (in the rotating frame). Scaling the independent variables by their natural values, that is, lengths by the corotation radius, $R_{\text{co}} \equiv (GM_*/\Omega^2)^{1/3}$ (with M_* the central star's mass and Ω its rotational angular velocity) and time by $1/\Omega$, the following blob equations of motion are found (Ultchin et al. 1997):

$$\ddot{x} = 2y + x - \frac{x}{R^3} - k_d(\mathbf{x}) [\dot{x} - (\dot{\mathbf{x}} \cdot \mathbf{b}) b_x], \quad (8)$$

$$\ddot{y} = -2x + y - \frac{y}{R^3} - k_d(\mathbf{x}) [\dot{y} - (\dot{\mathbf{x}} \cdot \mathbf{b}) b_y], \quad (9)$$

$$\ddot{z} = -\frac{z}{R^3} - k_d(\mathbf{x}) [\dot{z} - (\dot{\mathbf{x}} \cdot \mathbf{b}) b_z], \quad (10)$$

These constitute the nondimensional equations of motion for the cartesian components, in the *rotating frame*, of the blob trajectory $\mathbf{x}(t)$ and are thus ready to be incorporated into HYDISC (see in the next section). R , the cylindrical radius, is obviously $R \equiv (x^2 + y^2)^{1/2}$ and the calculation of \mathbf{b} is quite simple for an aligned dipole. For a tilted dipole, a somewhat more involved (but straight forward) calculation is needed.

The drag term has been written as k_d , the nondimensional version of K_d (of equation 6). The explicit form of this function, following from equations 6 and 7, brings out the physical meaning of the constant coefficient k appearing in front of the nondimensional spatially dependent part of the magnetic field

$$k_d(\mathbf{x}) = k (R/R_*)^{-3} [1 + 3(z/R)]^{1/2}, \quad (11)$$

which is

$$k = 2.82 \left(\frac{B_0}{100 \text{ G}} \right) \left(\frac{\rho_p}{10^{-10} \text{ g cm}^{-3}} \right)^{1/2} \left(\frac{l_b \rho_b}{100 \text{ g cm}^{-2}} \right)^{-1} \left(\frac{P_*}{10^6 \text{ s}} \right) \sim \frac{t_{\text{rot}}}{t_{\text{mag}}(R_*, 100 \text{ G})}. \quad (12)$$

Here reasonable (order of magnitude) estimates of the parameters for accreting T Tauri systems have been used to scale the relevant variables. $P_* \sim t_{\text{rot}}$ is the stellar spin period and B_0 the polar magnetic field strength. The disc density scaling value is estimated from models of standard accretion discs around T Tauri stars, using a representative accretion rates of $\dot{M} \sim 5 \cdot 10^{-8} M_{\odot} \text{ yr}^{-1}$ (Basri & Bertout 1989). The blob parameters are rather uncertain, but it is reasonable that the blob size is probably of the order of the vertical scale height in the disc while its density should be several orders of magnitude larger than that of the disc. This gives the value with which we scale $l_b \rho_b$. In any case, our results will be seen to depend

only on the parameter k (and several other quantities related to the numerical model) and hence on the particular combination given in equation 12.

Time-scale estimates can now be easily seen to demonstrate that for $k \sim 1$ the magnetic drag time-scale near the star (where $R \sim R_*$ and thus the contribution of the space dependent part, arising from eq. 11, is very close to 1) for a polar field of $\sim 100\text{G}$, denoted here by $t_{\text{mag}}(R_*, 100\text{G})$, is much larger than the dynamical time-scale there, since the latter is much shorter than t_{rot} (T Tauri stars are slow rotators). Thus we do not expect a significant effect near the star due to the magnetic drag in this case. Since the magnetic field decays (and thus the magnetic drag time scale grows) faster with R than the dynamical time-scale, the effect of the magnetic field on the motion will be small everywhere for $k \sim 1$

Let us examine now what happens at the corotation radius. From the functional dependence of the dipole field (eq. 11) we have the term $(R_{\text{co}}/R_*)^{-3} = (\Omega/\Omega_K)^2$, with the ratio of the Ω -s evaluated at the stellar surface. This term is of the order of 10^{-2} in T Tauri stars, but t_{rot} , by definition, is equal to the dynamical time scale at the corotation radius. If one chooses $k \sim 100$, a significant effect of the magnetic force at corotation is expected and obviously more so inside corotation. Thus we expect a significant modification of the inner accretion disc in this case.

These time-scale estimates provide the rationale for our choice of the k parameter range (or B_0 with all the other parameters constant) in the simulations (described in §4). Note that the viscous time-scale did not enter our considerations here. In accretion disc theory it is always assumed that this time-scale is much larger than the dynamical time-scale and consequently if the the magnetic time-scale approaches the dynamical one they are both much shorter than the viscous time scale. However, in regions where the magnetic time-scale is extremely long (far out in the disc, or even quite close in, if the field is weak enough) it might be even longer than the viscous time-scale and thus the magnetic drag would not interfere with the viscous evolution of the disc.

3 THE NUMERICAL METHOD

3.1 General considerations

To facilitate an accretion flow simulation in our system we adapt HYDISC, a numerical particle code originally written by Whitehurst (1988) to study accretion in CV, to the problem of a single central magnetic accretor (a T Tauri star). The introduction of the magnetic

interaction into the particles' equations of motion, using the DBA approach, has already been explained in the previous section. Our blobs are being considered as the particles of the particle scheme, utilized in HYDISC to simulate the hydrodynamical aspects of the flow, like pressure and viscosity. As it was already mentioned in the Introduction, similar schemes based on HYDISC have been designed for simulating accretion flows in magnetic CV (Wynn & King 1995; Wynn, King & Horne 1997) and also for investigating the outflows and spin evolution of an accreting T Tauri star (Pearson & King 1995).

Our calculation is, in principle, similar to the latter work because the gravitational effects of the companion star are removed from the code, however the purpose of this work and therefore the simulation details are quite different. We are interested in obtaining a steady-state structure of the disc itself and the spectral shape of the emitted radiation after the spin period of the central star has settled onto its equilibrium value. This calls for the determination of an appropriate spatial computational domain, a suitable particle injection scheme (initializing the calculation) and the need for a method to assess the temperature (and from it, the integrated spectrum) of the accreting matter.

The inner and outer boundaries of our *computational region* are the stellar radius, R_* , and the "escape" radius, R_{out} (which is a parameter typically set at $\sim 10 R_{\text{co}}$), respectively. Particles are injected into the computational domain (in a manner described below) and if during the course of the evolution they are found to leave this domain, they are removed from the calculation altogether. Once in the computational zone, each particle is subject to the field forces formulated explicitly in the rotating frame by the equations of motion 8 through 10. In addition, short-range forces, reflecting the interaction between adjacent particles and thus simulating the hydrodynamical aspect of the dynamics, are employed using the HYDISC version of the particle hydrodynamics approach (Whitehurst 1988). These forces are controlled by three parameters: C , determining the pressure force; Q , a constant of order unity and r_v , the "chaining" mesh size. Physically C is the sound speed, Q is in fact the coefficient of restitution of the particle-particle collisions and is less than 1 for inelastic collisions, which must be assumed to simulate viscous flows, and r_v is the viscous scale-length (for details, see Whitehurst 1988).

The fact that HYDISC separates the treatment of the long-range (field) forces from the short-range (hydrodynamical) ones makes this code convenient for application to our problem. Most changes are introduced in the field part (as explained in the previous section on the equations of motion) and in the initialization schemes, that is, particle injection

(see below), while the treatment of particle interactions remains essentially the same as in HYDISC, with an appropriate choice of the parameters.

The structure of HYDISC, as explained above, allows also to estimate, relatively easily, the energy dissipation (see below).

3.2 Particle injection and disc initialization

Our problem involves an accretion disc around a single star and thus the injection scheme has to be chosen accordingly. The disc around a T Tauri star is not being continuously replenished by an external stream, as is the case in discs fed by the secondary star in a close binary system, like a CV. This said, we still may chose between two distinct possibilities: a "burst" injection, in which all particles are injected simultaneously (or almost so) and a continuous injection. In both cases we have also to select the *spatial* distribution of the injected particles. Clearly, in order to obtain meaningful results the ultimate configuration should not depend on the initial conditions. Computation time limitations dictate that the computational zone must be limited (as well as the total number of particles). Thus, the seemingly best option, i.e. to continuously inject particles at a radius much larger than R_{co} and wait for the disc to be built up by viscosity, is prohibitive. We have adopted instead what we call a "modified burst" injection scheme.

The particles were injected at an equatorial ring around a radius R_{inj} with a Gaussian spread in the individual particles injection radii and a small Gaussian displacement out of the disc plane as well. Each particle was initially assigned an azimuthal Keplerian velocity plus a random contribution, appropriate for the local disc temperature. The temperature of the disc, used to calculate the above mentioned random contributions to the injected particles' velocities and the sound speed (and thus the constant C), was estimated using the analytical standard disc model. The actual formula which we have used is identical to formula 6 of PK:

$$T(r) = T(3) \left[\frac{27}{1 - 3^{-1/2}} r^{-3} (1 - \sqrt{r}) \right]^{1/4}, \quad (13)$$

where r is the radius in units of R_* and $T(3)$, is the temperature at 3 stellar radii, where true estimates are available (Basri & Bertout 1989). Although the temperature in our disc is somewhat different, this estimate actually influences only the pressure in the disc (in addition to the initial condition) and therefore the error it introduces should be negligible (see PK).

In order not to lose too quickly significant numbers of particles from the simulations, the "modified burst" scheme consisted of extending the burst duration to a finite (typically a few stellar rotation periods) time τ_b , with the injection rate decaying with time in a Gaussian manner. In addition, particles were added at a constant (but rather slow as compared to the burst) rate \dot{N}_{cont} so as to compensate for particles lost from the computational zone (accreted or expelled). The spatial distribution of the added particles was kept fixed in time. Thus the modified burst scheme actually gave rise to the following number of injected particles as a function of time (expressed here in units of the rotation period)

$$N_{\text{inj}}(t) = N_b(t) + \dot{N}_{\text{cont}} t, \quad (14)$$

where $N_b(t) = \int_0^t \dot{N}_0 \exp(-t_1^2/2\tau_b^2) dt_1$. Typically, in our simulations the total number of particles in the burst (i.e. $N_b(t = 3\tau_b)$ say) was between 5000 and 10000 and $\dot{N}_{\text{cont}} = 150$ particles per rotational period (see below).

3.3 Calculation of the emitted spectrum

With the present DBA scheme it is impossible to obtain a detailed thermal structure of the accretion flow and therefore we aim at approximating just the effect of the magnetic field on the emitted spectrum, *relatively* to the non-magnetic ($k = 0$) case. We assume that the disc is optically thick in the region of interest and that the energy dissipated in it by the viscous interaction is immediately locally radiated out in the vertical direction. These assumptions are essentially the same as in the standard Shakura & Sunyaev treatment of geometrically thin and optically thick accretion discs. What is different here is the fact that the viscous dissipation rate must be computed from the details of the numerical particle scheme and can not be found directly from the disc's viscous flow. As explained above, a part of the kinetic energy of the particles (blobs) is lost in collisions as these are inelastic ($Q < 1$). After dividing the computational zone into cells, by a two-dimensional grid in the disc plane, one can calculate the energy released in each cell ΔE_{ij} during a given time Δt , provided the *masses* of the particles are known. The composite spectrum can then be found by adding up the contributions of all the cells in the computational domain, with each cell assumed to contribute a black-body emission spectrum, corresponding to its effective temperature

$$T_{ij}^{\text{eff}} = \left(\frac{\Delta E_{ij}}{\Delta t A_{ij} \sigma} \right)^{1/4}, \quad (15)$$

where A_{ij} is the cell surface area and σ is the Stefan radiation constant.

As explained in §2 (see equations 11 and 12) we have lumped the unknown values of the blob properties into a single parameter and chosen a specific spatial dependence for it. Thus for a given value of the coefficient k , different combinations of the constituent parameters (and among them the blob’s mass) is allowed. Assuming some fixed average blob mass can thus give a spectral shape, which should be considered as a *qualitative* estimate and have a *relative* meaning, that is, the spectral shapes for different values of k can be perceived as an assessment of the effect of the magnetic field strength on the shape of the spectrum. In addition, since our computational zone does not include (due to computing time limitations) the extended outer portion of the disc, the results must be interpreted remembering this fact. In particular, since the outer cool parts of accretion discs contribute mainly to the long wavelength part of the emitted spectrum, our computed spectra clearly *underestimate* the spectrum strength for large λ (see below in Fig. 3).

4 THE SIMULATIONS

4.1 Simulation parameters

In choosing the parameters of the simulations we have tried to optimize the sometimes conflicting demands to obtain, on the one hand, meaningful results and on the other hand to limit, as much as possible, the CPU demands of the numerical calculations.

We have set the stellar parameters in all the simulations to be $M_* = M_\odot$, $R_* = 1.5R_\odot$, $P_* = 10^6 \text{ s} \sim 11 \text{ days}$, giving for the corotation radius $R_{\text{co}} \approx 1.5 \cdot 10^{12} \text{ cm} \sim 14R_*$. As explained before, the corotation radius serves as our length unit.

Experimenting with different injection radii (the location of the centre of the injection ring), we have found that with the injection scheme (14) an injection radius of $R_{\text{inj}} = 1.4R_{\text{co}}$ is effective in building up rather quickly an accretion disc, which does not differ essentially from the one resulting (after a longer calculation) from a larger injection radius. In these tests we have shut off the magnetic interaction, but remembered from previous works that the injection radius should not be too close to corotation. Consequently in all the simulations we have used this value of the injection radius, with a Gaussian spread of up to $\pm 0.1R_{\text{co}}$.

As discussed in the previous section, the parameters related to the particle scheme treatment of the pressure and viscosity include C , Q and r_v . We chose C to be equal to the isothermal sound speed, derived from the standard Shakura & Sunyaev disc temperature distribution. Q and r_v determine the viscous effects and have to be chosen with care. Q , the

restitution coefficient has a global effect on the simulation and since its reasonable values should lie between 0.5 and 1 ($Q < 0.5$ allows particle interpenetration and $Q = 1$ corresponds to elastic collisions). We have found that changing Q within the above mentioned range has only a small effect on the final quasi steady state, but it influences the length of the time until such a state is reached. Whitehurst (1988) reached a similar conclusion by experimenting with $Q = 0.6$ and 0.7 values in the original HYDISC code. Thus, wishing to shorten the simulation time, without, however, making the viscosity unphysically large, we have opted for $Q = 0.7$ and used this value in all our simulations, save for a few test cases.

The parameter r_v , setting the viscous interaction length scale, has a local effect on the simulation. When deciding on the range of variation for this parameter we have taken into account the fact that too small a value of r_v causes the viscous evolution time to be unacceptably long. In addition, because the number of cells in the computational range becomes large, one has to increase the number of particles in order to keep the particle treatment meaningful. Both effects increase the CPU time and we have found that for $r_v \lesssim 0.02$ we were unable to efficiently compute the disc evolution. On the other hand for r_v approaching the value of 0.1 the increase in viscosity causes the particles to clump together and the evolution becomes unrealistically viscosity dominated. Performing test calculations with no magnetic interaction ($k = 0$) we found that an initial ring injected around $1.4R_{\text{co}}$ viscously spreads to a structure very similar to a standard thin disc in a time of $\sim 100 - 300$ rotational periods when r_v is kept within the range $0.08 \geq r_v \geq 0.03$. Using such a calculation it is also possible to find what is the effective α (the viscosity coefficient in the Shakura & Sunyaev prescription) with a given choice of Q and r_v . A test calculation with $r_v = 0.05$ (in units of R_{co} , see below) and $Q = 0.7$ was very similar to the evolution of a ring of matter to as it is found from a standard exercise with an α viscosity (see e.g. Pringle 1981) value of ~ 0.1 .

The parameters k and r_v were varied in the different simulations. The range of the variation of k was chosen so as to correspond to polar stellar magnetic value of up to several kiloGauss (when the other parameters in k are set to their representative values, see equation 7) and r_v was chosen within the range mentioned above.

4.2 Results of representative cases

We have performed 12 full simulations of an accretion disc in an aligned dipole magnetic field for different choices of the pair of parameters k and r_v . The simulations were initialized using the injection scheme described in equation 14 with parameters chosen so as to insure that the number of particles does not drop below $\sim 10^4$ during the simulation. The simulations were continued until a quasi-steady configuration was achieved, that is, no significant changes of the structure were observed over a significant time (see below). We have chosen to describe here in some detail the simulations with $r_v = 0.05$ (simulation group 3 in our list), that is, with the viscosity strength chosen in the middle of its feasible range. As discussed in the previous section this choice corresponds to an effective $\alpha \sim 0.1$. Three runs were performed for different values of the magnetic interaction strength ($k = 0, 10, 100$), where the non-magnetic case ($k = 0$) was run to serve as reference, in particular for the spectra, which have quantitative meaning only in comparison to each other (as explained before).

These three runs were all allowed to continue for a total simulation time of $250P_*$. A quasi-steady state was achieved already after approximately half of this time. The CPU time requirement for each run, with the number of particles kept at $\sim 10^4$ (the accreted and ejected particles were replenished as explained above), was about 100 hours on a Sun ULTRA 2 workstation, when the program was coded in C, to increase its efficiency. In Fig. 1 we show the surface number density of the particles (a quantity proportional to the disc surface mass density, customarily called Σ) as a function of radius for the three values of k . Note that in the innermost and outermost parts of the disc, regions in which the surface density curves are dashed, the number of particles is too small to render the result to be quantitatively reliable. We also plot on this graph the analytical result, arising from a standard thin disc formula with inner cutoff (see below). This is represented by the fully dashed curve, which follows the $k = 100$ case for most of the range.

From this figure it is evident that the effect of the magnetic field on the disc structure is important, as it significantly modifies the functional dependence of the surface density on the radius. For $k = 0$ (no magnetic field) the particles form a rather "collapsed" with its density growing sharply towards the central object. This is so because our simulations were tailored for the high k case and therefore the particle injection rate was too small for the buildup of a steady disc in a small k case. A growing magnetic field strength has a dynamical effect on the disc. As could be expected from a previous study, in which individual

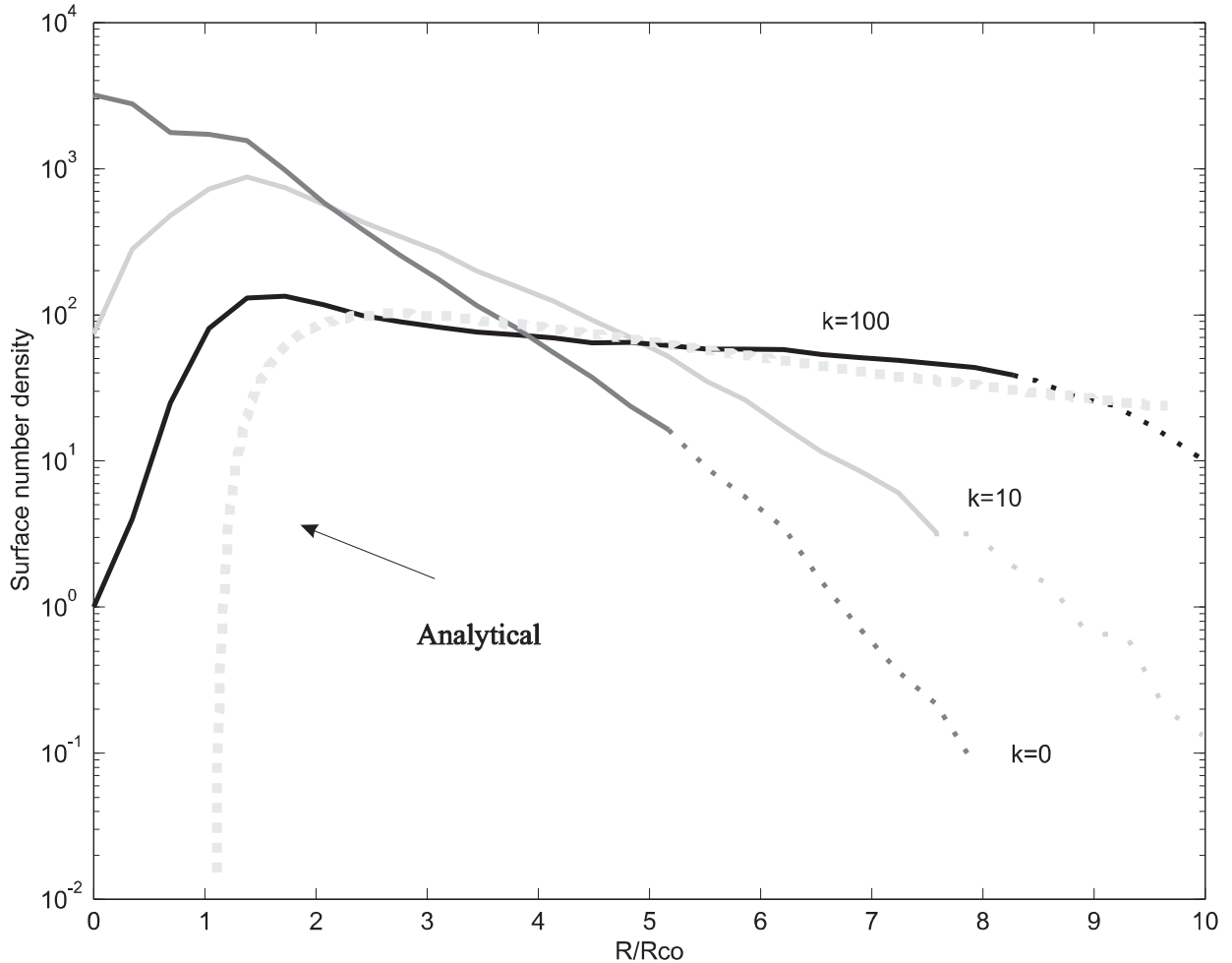


Figure 1. Surface number density as a function of radius (in units of R_{co}) for $r_v = 0.05$ (simulation 3) and three values of k . The number of particles in the innermost and outermost regions, denoted by dashed portions of the curves, is too small to render the results to be quantitatively reliable there. The fully dashed curve is an analytical result of a disc truncated at R_{co} .

orbits of particles were calculated (Ultchin et al. 1997), and from the DBA simulations of PK, the magnetic interaction drags blobs residing inside corotation towards the star and pushes out blobs whose orbits are outside corotation. These effects are modified here by the fact that the dipole magnetic field decays outwards and by the interblob interactions. The combined effect is a significant depletion of blobs close to the star (a "hole") and an increase of density at large radii (a "flattening" of the functional dependence of the surface density on radius). The size and depth of the hole and the extent of the flattening of the surface density obviously depend on k , That is, on a combination of the disc density (which depends on the accretion rate) and the strength of the magnetic field.

Analytic estimates of the hole radii at spin equilibrium, as given by Cameron and Campbell (1993), predict that the disc should end abruptly close to the corotation radius (but depending also on the fastness parameter of the star). Our numerical results do not yield an

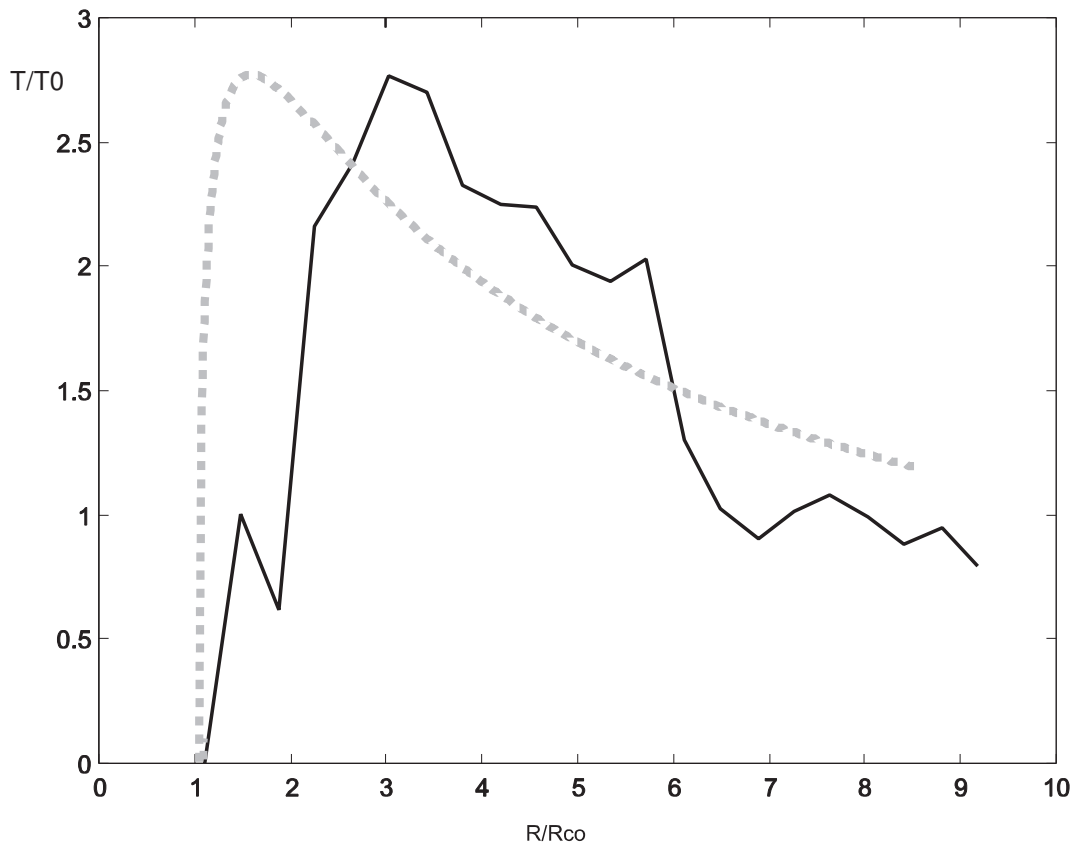


Figure 2. The effective temperature (in arbitrary units) as a function of radius (in units of R_{co}) for $r_v = 0.05$ (simulation 3) and $k = 100$. The dashed curve is the analytically obtained temperature distribution of a classical accretion disc, cut off inside at $R_{\text{in}} = R_{\text{co}}$ (see 17)

abrupt disc termination, but the value of $\sim R_{\text{co}}$ is certainly consistent with these results. In the following comparisons of our results to analytical solutions we have used this value of the inner cutoff radius, that is, the analytical formulae giving rise to the fully dashed curves in Figs. 1 and 2 (see below) result from

$$\Sigma(R) = \frac{\dot{M}}{3\pi\nu} \left[1 - \sqrt{R_{\text{co}}/R} \right] \quad (16)$$

and

$$T^4(R) = \frac{3GM\dot{M}}{8\pi R^3\sigma} \left[1 - \sqrt{R_{\text{co}}/R} \right], \quad (17)$$

with the values of ν and \dot{M} chosen appropriately, from our calculation, so as to enable the comparison.

If Fig. 2 we show the comparison of the analytical (effective) temperature distribution as given in (17) with the numerical result for the case of $k = 100$, when the outer parts of the disc resemble most the analytical result (see Fig. 1). The lack of the inner, hottest,

part in the numerical results is apparent. In these calculations the method described in §3.3 was used to monitor the energy dissipation during the simulations and calculate the discs temperature structures and their spectra. The spectral flux distributions (λF_λ) in the three cases of k depicted in Fig. 1 are displayed in Fig. 3.

It is apparent from the figure that with increasing k the spectral distribution of the emitted radiation is shifted towards longer wavelengths. This trend is quite clear since as we have seen in Fig. 1 and 2, the hottest material, which resides close to the star, is significantly depleted by the magnetic interaction. In addition, as a result of the increase of the surface density in the outer cooler parts, the contribution to the long-wavelength part of the spectrum is more prominent. We stress once again that the temperature calculation and hence that of the spectrum suffers from the fact that the *mass* of the blobs is essentially unknown, so that the results displayed in Fig. 3 are of a qualitative nature and their value is mainly in uncovering the trend of the spectral behaviour. In addition, computer time limitations do not allow us to extend the calculation to the outer parts of the disc (here, in simulation 3 we have $R_{\text{out}} = 10R_{\text{co}}$). Thus the spectral energy distributions in Fig. 3 fail to account for the cool material lying outside the outer limit of the computational zone and which should have an effect of increasing the strength at long wavelengths. Since the disc is more extended for large k this effect should matter the most in the strongly magnetic case. The actual structure of the accretion disc for the three values of k can be seen in Fig. 4, in which maps of the the surface density and temperature are shown.

From the examination of Fig. 3 and the above considerations it is thus reasonable to conclude that the magnetic interaction, at least as it is dealt with in this work, tends to flatten the spectrum for long wavelengths, consistently with the observed IR excess mentioned in the Introduction.

The results of all the other simulations (i.e. the ones with a different value of the viscosity scale parameter r_v) are similar to the ones described above and thus the conclusions are similar. The actual value of r_v has only a little effect on the final (i.e. quasi-steady) surface density and temperature distribution, as long as this value is within the calculation feasibility range (see above). The difference is in the time that has to pass until the configuration settles down. This is understandable as the evolution time is essentially the viscous time scale and the latter decreases with increasing r_v .

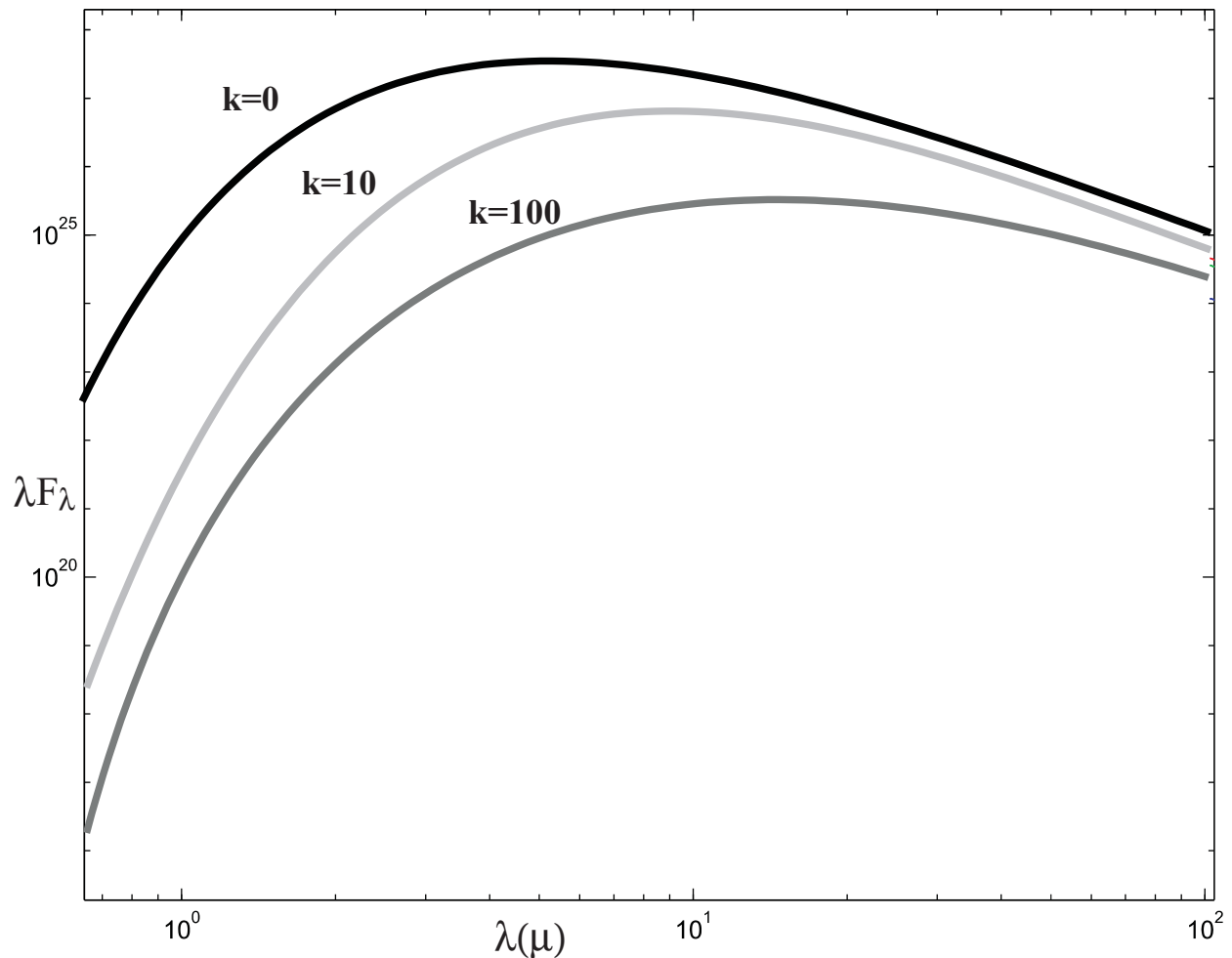


Figure 3. Spectra of the accretion discs in simulation 3. λF_λ in arbitrary units (see text) is plotted as a function of wavelength λ in microns for three values of the magnetic interaction parameter k .

4.3 Effects of special magnetic field geometry

We have performed, in addition to the simulations described above in which the magnetic field was that of an aligned dipole, two simulations with different magnetic configurations. In the first one we have used a magnetic dipole whose axis was tilted to the disc axis and in the second one a "dipole slice" (see below) was introduced in order to estimate the effects of a localised magnetic field configuration.

4.3.1 Tilted dipole

A single simulation was performed with $r_v = 0.05$; $k = 100$, that is, similar to one of the simulations described above, but with the magnetic dipole axis tilted at an angle of 45° to the disc axis. The results show relatively few changes as compared to the aligned dipole case. There was almost no perturbation of the disc matter, relatively to the aligned dipole case, far out of the corotations radius. This is understandable since the blobs orbiting at these

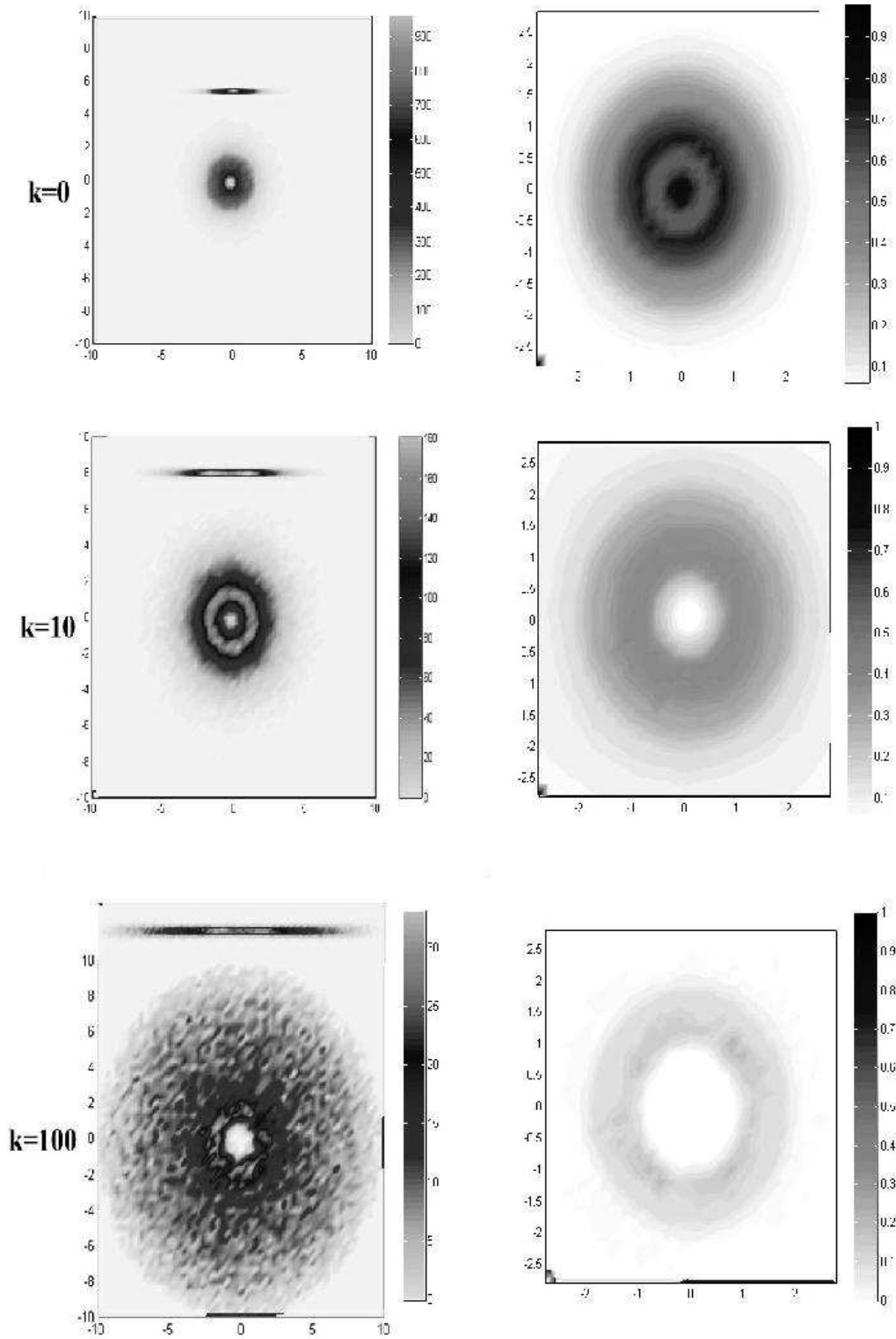


Figure 4. Surface density (left panels) and temperature (right panels) maps for simulation 3 ($r_v = 0.05$) for the three values of the magnetic interaction strength. Arbitrary units are used and in the surface density maps a side view of the disc is also given, in the upper part of each panel. Surface density (left panels) and temperature (right panels) maps for simulation 3 ($r_v = 0.05$) for the three values of the magnetic interaction strength. Arbitrary units are used and in the surface density maps a side view of the disc is also given, in the upper part of each panel.

positions experience in this case a magnetic field whose direction oscillates with the period of the stellar rotation (which is considerably shorter than the blob’s Keplerian period). Thus, it is expected that the blobs actually react to the average magnetic field, i.e. behave in a similar way as in the aligned dipole case.

This expectation is wrong for blobs close to and inside corotation. Indeed, their motion should be channeled there by the magnetic field. This effect could not be observed in our simulations since the density of the particles in the magnetosphere, above the disc plane, is very small. A very high number of particles or alternatively an extremely strong magnetic field is needed in order to resolve, in our type of calculation, the particle flow along field lines. This remark obviously applies to the aligned dipole case as well.

4.3.2 Dipole slice

To simulate the case in which the actual stellar magnetic field resembles a localized loop, similar to the case studied by PK, we have used a ”slice” of the aligned dipole, with Gaussian fall-off in strength in both the radial coordinate R and the azimuthal angle θ . Thus we have performed a simulation with $r_v = 0.05$; $k = 500$ and with the magnetic field centered on the position R_0, θ_0

$$B_{\text{slice}} = B_{\text{dipole}} \exp[-(\theta - \theta_0)^2/2d_\theta^2] \exp[-(R - R_0)^2/2d_R^2], \quad (18)$$

where B_{dipole} is a dipole field (see the functional dependence in equation 6 and d_R, d_θ are the radial and angular Gaussian fall-off scales in the radial and azimuthal directions. In the simulation we have chosen $R_0 \sim R_{\text{co}}$, consistently with the findings of KR that this should be the equilibrium configuration.

The results clearly depend on d_R and d_θ . When we chose $d_R \sim R_{\text{co}}$, the disc beyond R_{co} resembled the non-magnetic case ($k = 0$), since the field is practically zero there. Closer to corotation and inside it, the density distribution looked like that of a full but *weaker* dipole, since the dipole slice field effectively acts on the orbiting blobs only along a fraction $\sim d_\theta/2\pi$ of the blob’s orbit.

5 SUMMARY AND CONCLUSIONS

The most prominent feature of our simulation results is the formation of a low density region (a hole) in the inner part of the disc as a result of the magnetic interaction. In addition, the density distribution becomes more spread out, as the slope of $\log \Sigma(R)$ decreases with

increasing k . This behaviour is typical and essentially qualitatively independent of all the other parameters. Although the "hole" is the more noticeable feature (see e.g. the density maps in Fig. 4), it is less significant to overall observable features than the global change in the density distribution.

We have also seen, by comparing our calculations with what can be expected from analytical results, that we uncover some features (like the absence of hot material close to the inner hole) which can not be obtained from just classical disc models with a hole inside.

Due to computer power restrictions we were unable to achieve a high enough resolution, so as to see the accretion flow along the field lines and outflows from the system. In addition we were able to simulate only a limited portion of the disc and thus the calculations of the spectrum reveal only the general trend. This trend, resulting from the flattening of the surface density distribution, was always to shift emission power toward longer wavelengths. The flattening of λF_λ is most apparent near its maximum and it is reasonable that were it not for the close (computational) cutoff in R , the shape would remain flat to longer wavelengths. We propose therefore that the IR excess in T Tauri stars can be attributed to magnetic interaction, which modifies the functional dependence of the surface density in the surrounding discs.

Existing models attempting to explain the IR excess in T Tauri stars fall into two distinct categories: those invoking geometrical factors and others, proposing energy dissipation mechanisms operating preferably in the outer parts of the disc. Our model suggests a correlation between the spectrum flatness and the magnetic field strength, appears to be quite robust (practically any shape of the magnetic field would do) and does not require assumptions about flared shapes of discs or unusual energy dissipation modes. At this stage, the results of our calculation provide little more than support for a *qualitative* promising idea. As it was mentioned in the Introduction, it is possible to apply a similar prescription to the case in which the magnetic field penetrates the disc. We can reasonably expect that the results of such a calculation should not be too different, at least qualitatively, from the ones presented in this paper. It appears that all that is required is magnetic field lines imparting a torque on the gas, which changes in sign as we cross the corotation radius.

Significant results for both models of the magnetic interaction can be achieved in high resolution (significantly larger number of particles). However, to extend the idea into a reliable quantitative model, full multidimensional MHD simulations, including radiative transfer, have to be ultimately performed.

ACKNOWLEDGMENTS

We thank Giora Shaviv for helpful remarks and suggestions. Yigal Ultchin acknowledges the hospitality of the Astronomy Group at Leicester University and the financial support extended to him at the Technion. This research was supported by grants from the Israel Science Foundation, the Helen & Robert Asher Research Fund and by the Fund for the Promotion of Research at the Technion. We would also like to thank the referee, whose insightful comments helped considerably in improving this paper.

REFERENCES

- Aly J.J., Kijpers J., 1990, *A&A*, 227, 473
Armitage P.J., Clarke C.J., 1996, *MNRAS*, 280, 458
Basri G., Bertout C., 1989, *ApJ*, 341, 340
Beckwith S.V.W., Sargent A.I., Chini R.S., Güsten R., 1990, *AJ*, 99, 924
Bertout C., 1989, *ARA&A*, 27, 351
Cameron A.C., Campbell C. G., 1993, *A&A*, 274, 309
Drell S., Foley H.M., Ruderman M.A., 1965, *J. Geophys. Res.*, 70, 3131
Frank Y., King A.R., Raine D.J., 1992, *Accretion Power in Astrophysics*, 2nd edn., Cambridge University Press, Cambridge
Hartmann L., Hewett R., Calvet N., 1994, *ApJ*, 426, 669
Hartmann L., 1998, *Accretion Processes in Star Formation*, Cambridge Univ. Press, Cambridge
King A.R., 1993, *MNRAS*, 261, 144
King A.R., Regev O., 1994, *MNRAS*, 268, L69 (KR)
King A.R., Wynn G.A., 1999, *MNRAS*, 310, 203
Königl A., 1991, *ApJ*, 370, L39
Lin D.N.C., Papaloizou J.C.B., 1996, *ARA&A*, 34, 703
Lynden-Bell D., Pringle J.E., 1974, *MNRAS*, 168, 603
Papaloizou J.C.B., Lin D.N.C., 1995, *ARA&A*, 33, 905
Pearson K.J., King A.R., 1995, *MNRAS*, 276, 1303 (PK)
Pringle J.E., 1981, *ARA&A*, 19, 137
Shakura N.I., Sunyaev R.A., 1973, *A&A*, 24, 337
Ultchin Y., Regev O., Bertout C., 1997, *ApJ*, 486, 397
Whitehurst R., 1988, *MNRAS*, 233, 529
Wynn G.A., Leach R., King A.R., 2001, (submitted to *MNRAS*)
Wynn G.A., King A.R., 1995, *MNRAS*, 275, 9
Wynn G.A., King A.R., Horne K., 1997, *MNRAS*, 286, 436